Multiple ordered phases in the filled skutterudite compound PrOs$_4$As$_{12}$

W. M. Yuhasz, N. P. Butch, T. A. Sayles, P.-C. Ho, J. R. Jeffries, T. Yanagisawa, N. A. Frederick, and M. B. Maple
*Department of Physics and Institute for Pure and Applied Physical Sciences, University of California San Diego,
La Jolla, California 92093, USA*

Z. Henkie and A. Pietraszko
Institute of Low Temperature and Structure Research, Polish Academy of Sciences, 50-950 Wrocław, Poland

S. K. McCall, M. W. McElfresh, and M. J. Fluss
Lawrence Livermore National Laboratory, P. O. Box 808, Livermore, California 94550, USA

Magnetization, specific heat, and electrical resistivity measurements were made on single crystals of the filled skutterudite compound PrOs$_4$As$_{12}$. Specific heat measurements indicate an electronic specific heat coefficient $\gamma \sim 50$–200 mJ/mol K^2 at temperatures 10 K $\leq T \leq 18$ K, and ~ 1 J/mol K^2 for $T \leq 1.6$ K. The combined measurements reveal the presence of two, or possibly three, ordered phases at temperatures below ~ 2.3 K and in fields below ~ 3 T. The low temperature phase displays antiferromagnetic characteristics, while the nature of the ordering in the other phase(s) has yet to be determined.

PACS number(s): 75.30.Kz, 71.27.+a

The filled skutterudite compounds, with the formula MT_4X_{12} (M=alkali metal, alkaline-earth, lanthanide, or actinide; T=Fe, Ru, or Os; and X=P, As, or Sb), display a wide variety of strongly correlated electron phenomena.[1–3] Of particular interest are the Pr-based filled skutterudites. The physical properties of these compounds are dominated by the ground state and the low lying excited state of the Pr^{3+} ion in the crystalline electric field (CEF), and the hybridization of the Pr $4f$ states with the ligand states of the surrounding Sb ions that compose the atomic cage within which each Pr^{3+} ion resides. A variety of correlated electron phenomena have been observed in the Pr-based filled skutterudites: conventional (BCS) and unconventional superconductivity, magnetic order, quadrupolar order, metal-insulator transitions, Kondo phenomena, heavy fermion behavior, and non-Fermi-liquid behavior. A prime example of this diversity is seen in the compound PrFe$_4$P$_{12}$, which undergoes a transition to an ordered state below 6.5 K that was originally thought to be antiferromagnetic (AFM) in nature,[4] but was later identified with antiferroquadrupolar (AFQ) order.[5,6] The suppression of this AFQ ordering in magnetic fields results in the formation of a heavy Fermi liquid state above the quadrupolar quantum critical point (QCP).[7,8,5] Below 1 K, a possible high field ordered phase between 8 and 12 T has also been observed in a limited angular range around the [111] direction.[9] One of the most interesting Pr-based materials is the compound PrOs$_4$Sb$_{12}$, which exhibits unconventional superconductivity, involving heavy fermion quasiparticles, below a critical temperature $T_c = 1.85$ K.[10–12] The superconducting state breaks time reversal symmetry,[13] appears to consist of several distinct superconducting phases,[12,14,15] and may have point nodes in the energy gap,[14,16,17] while between 4.5 and 16 T and below ~ 1 K, an ordered phase is observed that has been identified with AFQ order.[12,16,18,19] This suggests that the extraordinary normal and superconducting properties of PrOs$_4$Sb$_{12}$ may be associated with the proximity to a field-induced quadrupolar QCP, in accord with previous conjectures.[10–12]

Unlike the Pr-based filled skutterudite phosphides and antimonides, the arsenides have not been investigated in much detail. These materials provide an opportunity to discover other examples of strongly correlated electron behavior displayed by the Pr-based filled skutterudites. In this paper, we present an investigation of the physical properties of PrOs$_4$As$_{12}$ single crystals. These measurements reveal that PrOs$_4$As$_{12}$ is a Kondo lattice compound with an enhanced electronic specific heat coefficient γ of ~ 50–200 mJ/mol K^2 at temperatures 10 K $\leq T \leq 18$ K, and ~ 1 J/mol K^2 for $T \leq 1.6$ K. Multiple ordered phases are observed below 2.3 and 3.2 T; at least one of which appears to be AFM in nature.

Single crystals of PrOs$_4$As$_{12}$ were grown from elements with purities $\geq 99.9\%$ by a molten metal flux method at high temperatures and pressures, the details of which will be reported elsewhere.[20] After removing the majority of the flux by distillation, PrOs$_4$As$_{12}$ single crystals of an isometric form with dimensions up to ~ 0.7 mm were collected and cleaned further in acid to remove any Pr impurity phases from the surfaces. X-ray powder diffraction measurements were performed with a Rigaku D/MAX B x-ray machine on a powder prepared by grinding several single crystals along with a high purity Si(8N) standard. The crystal structure of PrOs$_4$As$_{12}$ was determined by x-ray diffraction on a crystal with a regular octahedral shape and dimensions of $0.12 \times 0.12 \times 0.12$ mm. A total of 5158 reflections (583 unique, $R_{int} = 0.1249$) were recorded and the structure was resolved by the full matrix least squares method using the SHELX-97 program with a final discrepancy factor $R1 = 0.0462$ [for $I > 2\sigma(I)$, $wR2 = 0.1124$].[21,22]

Magnetization M measurements for temperatures 0.4 K $\leq T \leq 10$ K and magnetic fields -5.5 T $\leq H \leq 5.5$ T were made in a ^{3}He Faraday magnetometer. A mosaic of 27 crystals, with a total mass of 27 mg, was measured with the [111]

TABLE I. Atomic coordinates, displacement parameters, and occupancy factors for $PrOs_4As_{12}$. U_{eq} is defined as one-third of the trace of the orthogonalized U_{ij} tensor.

Atom	x	y	z	U_{eq} ($Å^2 \times 10^3$)	Occupancy factor
Os	0.25	0.25	0.25	4(1)	1.00(2)
As	0	0.3485(1)	0.1487(1)	7(1)	0.96(2)
Pr	0	0	0	16(1)	0.97(2)

axis of the crystals nominally aligned parallel to H. Measurements of $M(T,H)$ were also performed using a Quantum Design Magnetic Properties Measurement System (MPMS) in H up to 5.5 T for 1.7 K $\leq T \leq$ 300 K. Four-wire ac electrical resistivity $\rho(T)$ measurements were made for 2 K $\leq T \leq$ 300 K in a Quantum Design Physical Properties Measurement System (PPMS) using a constant current of 1–10 mA, and for 0.06 K $\leq T \leq$ 2.6 K in a ^{3}He-^{4}He dilution refrigerator with a constant current of 300 μA. Measurements of $\rho(T)$ at various pressures P up to $\sim$23 kbar were made down to 1 K in a ^{4}He cryostat using a BeCu piston-cylinder clamp. Specific heat $C(T)$ measurements on $PrOs_4As_{12}$ were performed for 0.6 K $\leq T \leq$ 35 K at the University of California San Diego (UCSD) in a semiadiabatic ^{3}He calorimeter on a collection of single crystals with a total mass of 49 mg. Additional $C(T)$ measurements for 0.4 K $\leq T \leq$ 20 K were performed at Lawrence Livermore National Laboratory (LLNL) in a Quantum Design ^{3}He PPMS.

An analysis of the x-ray powder diffraction pattern indicates single phase $PrOs_4As_{12}$ with no major impurity peaks. A unit cell parameter $a = 8.5319(11)$ Å was determined, in excellent agreement with an earlier measurement[23] of $a = 8.5311(3)$ Å. Single crystal structural refinement shows that the unit cell of $PrOs_4As_{12}$ has the $LaFe_4P_{12}$-type structure ($Im\bar{3}$ space group) with two formula units per unit cell, and $a = 8.520(1)$ Å. Other crystal structure parameters are summarized in Table I. The displacement parameter U_{eq} represents the average displacement of an atom vibrating around its lattice position and equals its mean-square displacement along the Cartesian axes. The displacement parameters determined for $PrOs_4As_{12}$ show behavior that is typical of the lanthanide filled skutterudites.[24,25] Table I also indicates that the Pr site in $PrOs_4As_{12}$ can be assumed to be fully occupied since there is a $\sim$2% uncertainty in the occupancy factors.

The dc magnetic susceptibility $\chi_{dc}(T)$, measured in $H = 0.05$ T along the [111] direction, for 0.4 K $\leq T \leq$ 10 K, is shown in Fig. 1(a). The clear peak in the $\chi_{dc}(T)$ data suggests an AFM transition at $T = 2.3$ K. Figure 1(b) displays χ_{dc}^{-1} vs T in $H = 0.1$ T between 2 and 300 K. Above 50 K, the data are well-described by a Curie-Weiss law with an effective moment $\mu_{eff} = 3.81 \mu_B$/f.u. and a Curie-Weiss temperature $\Theta_{CW} = -25.8$ K. Below 20 K, $\chi_{dc}^{-1}(T)$ can be described by a different Curie-Weiss law, with $\mu_{eff} = 2.77 \mu_B$/f.u. and $\Theta_{CW} = 0.44$ K [Fig. 1(b) inset]; this behavior is consistent with CEF effects, as will be discussed later. The value of μ_{eff} derived from the high temperature (above 50 K) Curie-Weiss fit is larger than the theoretical Pr^{3+} free-ion value of
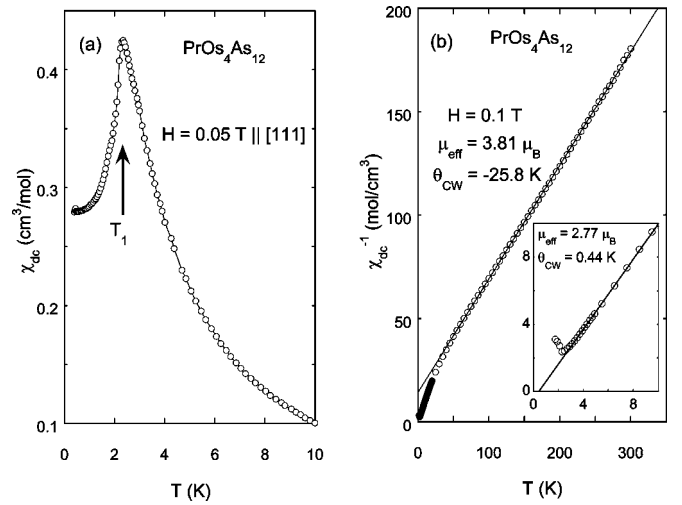

FIG. 1. (a) Magnetic susceptibility χ_{dc} vs T, indicating a magnetic transition at 2.3 K. (b) Inverse magnetic susceptibility χ_{dc}^{-1} vs T. The line represents a Curie-Weiss law, fit to the data above 50 K. The inset shows the low-T behavior of $\chi_{dc}^{-1}(T)$ along with a different Curie-Weiss law fit (see text).

$\mu_{eff} = 3.58 \mu_B$/f.u. A similar $\mu_{eff} = 3.84 \mu_B$/f.u. was also found for $PrRu_4P_{12}$.[26] In contrast, $PrOs_4Sb_{12}$ displays an effective moment of $2.97 \mu_B$/f.u.,[11] while both $PrOs_4P_{12}$ and $PrFe_4P_{12}$ display effective moments close to the Pr^{3+} free-ion value.[4,26] The larger-than-expected moment may be due to an unaccounted-for constant Pauli paramagnetic contribution. When a constant contribution χ_0 of $\sim 5.5 \times 10^{-4}$ cm^3/mol is assumed, which is consistent with a value of 5.16×10^{-4} cm^3/mol found for $LaFe_4P_{12}$,[27] the effective moment estimated from a Curie-Weiss law fit approaches the Pr^{3+} free-ion value with $\Theta_{CW} = -12.5$ K. The values of μ_{eff} and Θ_{CW} for the low temperature (below 20 K) Curie-Weiss law fit remain unchanged when the $\chi_{dc}(T)$ data are corrected for this value of χ_0.

Low-T $M(H)$ data taken with H parallel to [111] are shown in Fig. 2. An inflection point at low H is evident, along with two kinks in $M(H)$ (denoted H_1 and H_2) which are suppressed toward lower fields with increasing T. The inset of Fig. 2 shows the evolution of $M(H)$ from higher temperatures down to the ordering transition temperature. No magnetic hysteresis was observed. Features corresponding to H_1 and H_2 are found in $M(T)$ in constant H. With increasing H, a peak in $M(T)$ [labeled as T_1 in Fig. 1(a)] shifts towards $T = 0$ K, while a kink in $M(T)$ at higher T (denoted T_2) becomes apparent, splits off from T_1, and eventually also moves towards $T = 0$ K.

Specific heat $C(T)$ measurements on $PrOs_4As_{12}$ in zero field (Fig. 3) display two clear features: a slight shoulder at $T_2 \approx 2.3$ K, on the high temperature side of a well-defined peak at $T_1 \approx 2.2$ K. Zero-field measurements made at LLNL show similar behavior [Fig. 3 inset (b)], except that in the LLNL experiment, the peak at T_1 was further resolved into two distinct features separated by $\sim$0.02 K. This additional feature may indicate an additional transition or it may be due to a variation in composition among the measured crystals. At the lowest temperatures, there is a slight upturn in $C(T)$
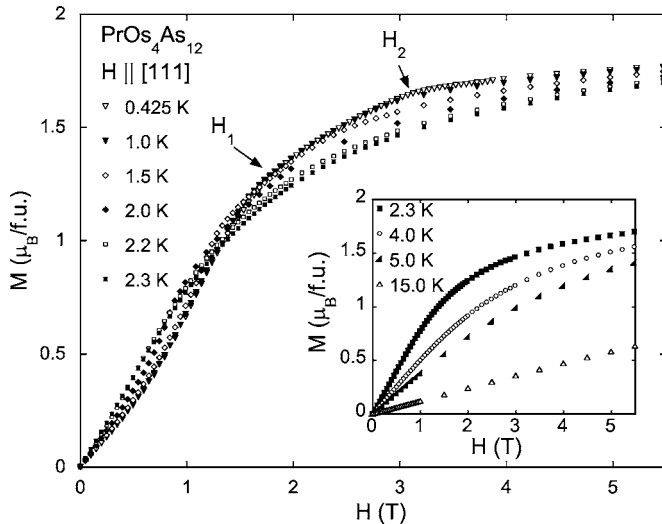
FIG. 2. Magnetization M vs H isotherms at several values of T. Features in $M(H)$ at constant T, with H_1 and H_2 defined by a kink in $M(H)$, are illustrated for $T = 0.425$ K. The inset shows $M(H)$ at higher temperatures.

associated with a nuclear Schottky anomaly. The low-T specific heat can be described by four contributions, $C(T) = C_n(T) + C_e(T) + C_l(T) + C_m(T)$, which are the nuclear Schottky, electronic, lattice, and magnetic terms, respectively. At higher temperatures, $C_m(T)$ and $C_n(T) \approx 0$, and the specific heat is dominated by the electronic and lattice terms. In Fig. 4(a), a fit of $C/T = \gamma + \beta T^2$ in the range $10 \text{ K} \leqslant T \leqslant 18$ K reveals an enhanced $\gamma \approx 200$ mJ/mol K^2 and, from β, a Debye temperature $\Theta_D \approx 260$ K. To analyze the specific heat in the ordered state, the three terms of the specific heat after subtraction of the lattice contribution (using $\Theta_D \approx 260$ K), $\Delta C(T) = C_n + C_e + C_m$, were assumed to have the following forms: $C_n(T) = A/T^2$, $C_e(T) = \gamma T$, and $C_m(T) = BT^n$. Using these equations, fits of $\Delta C T^2 = A + \gamma T^3 + BT^{n+2}$ were
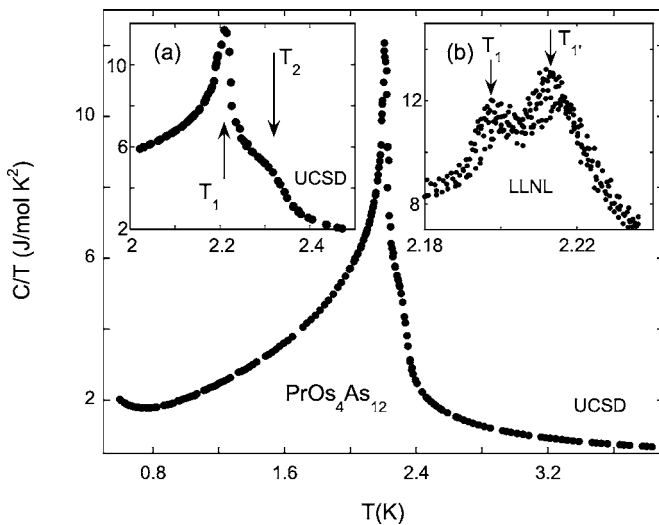

FIG. 3. Specific heat C divided by T vs T (UCSD data). Inset (a) shows the transitions at T_1 and T_2 in more detail (UCSD data). Inset (b) shows the apparent resolution of the transition at T_1 into two transitions at T_1 and T_1' (LLNL data).
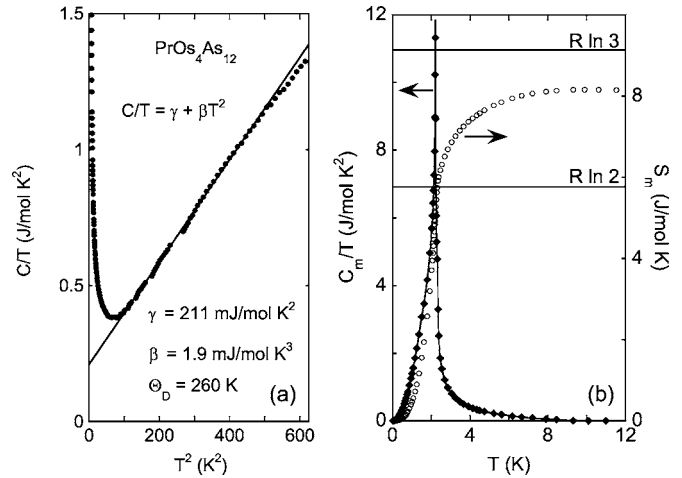

FIG. 4. (a) Zero field C/T vs T^2, with a linear best fit yielding the enhanced γ and value of Θ_D given in the figure. (b) Magnetic entropy S_m determined from the specific heat after the zero field lattice and electronic contributions to the specific heat were subtracted.

performed for $T < 0.6 T_1$. The best fit results in a nuclear Schottky coefficient $A = 128$ mJ K/mol and an exponent in the power-law term of $n = 3.2 \pm 0.1$, close to the expected value of $n = 3$ for AFM spin waves. The electronic specific heat coefficient γ is strongly enhanced, with a value near 1 J/mol K^2. A temperature dependent γ is not uncommon and has been observed in numerous compounds that exhibit heavy fermion behavior.[29] The value of 260 K for Θ_D is consistent with other filled skutterudite arsenides with typical values ranging from 230 K (LaRu$_4$As$_{12}$) to 340 K (PrRu$_4$As$_{12}$).[30,31] The magnetic entropy $S_m(T)$ was calculated from the specific heat by integrating $C_m(T)/T$ with temperature [Fig. 4(b)], resulting in an entropy release of 90% $R \ln 3$ that levels off by 8 K, a value consistent with a triply degenerate ground state. The reduction of the entropy from a full $R \ln 3$ is presumably due to the hybridization of the localized $4f$ and itinerant electron states, as is observed for PrOs$_4$Sb$_{12}$, where the entropy is apparently transferred from the localized $4f$ states to the conduction electron states.

The electrical resistivity $\rho(T)$ was measured in the range $0.06 \text{ K} \leqslant T \leqslant 300$ K (Fig. 5). Kondo lattice behavior is evident, as $\rho(T)$ decreases with decreasing T down to $T_{min} \approx 16.5$ K and then increases until ~ 5.5 K, where the resistivity drops due to the onset of the ordered state. Measurements in high magnetic fields can be analyzed in terms of a single ion Kondo model for an impurity effective spin of 1, yielding an estimate of T_K on the order of 1 K.[28] A small T_K with respect to the ordering temperature (~ 2.3 K) prohibits the observation of T^2 dependence of $\rho(T)$. Measurements of $\rho(T)$ under P up to ~ 23 kbar between 1 and 300 K revealed no significant P dependence.

As mentioned earlier, features in the $\chi_{dc}(T)$ data reflect CEF effects. Although the true crystal symmetry of the filled skutterudites is tetrahedral T_h, it is a close approximation in zero field to consider cubic O_h symmetry. In a CEF with O_h symmetry, the ninefold degenerate Pr^{3+} $J = 4$ multiplet is split into a Γ_1 singlet, a Γ_3 doublet, and Γ_4 and Γ_5 triplets. The
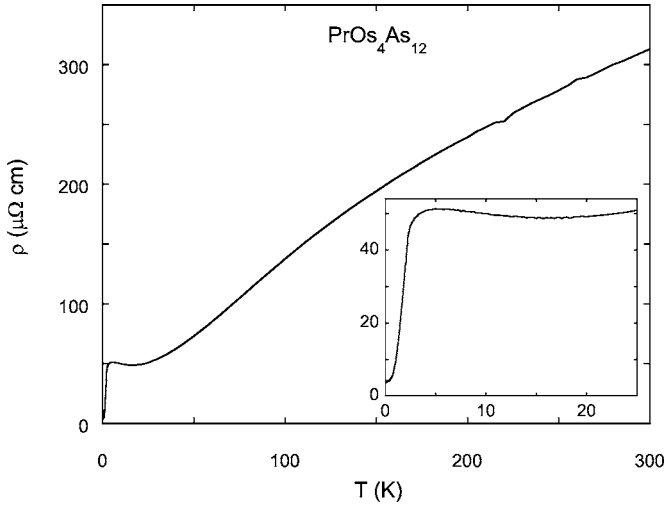
FIG. 5. Electrical resistivity ρ vs T from 2 to 300 K. The inset shows $\rho(T)$ from 0.06 to 25 K.

low-T calculated effective moment of $2.77\mu_B$/f.u. is indicative of a Γ_5 ground state, which has a theoretical effective moment of $2.83\mu_B$/f.u. In addition, $M=1.68\mu_B$/f.u. at 2 K and 5.5 T, a value much less than the full $3.2\mu_B$/f.u. saturated moment expected for a Pr^{3+} free ion, but more consistent with the $2.0\mu_B$/f.u. expected for a Γ_5 ground state. Reasonable CEF fits to the $\chi_{dc}(T)-\chi_0$ data (not shown) can be made using a CEF splitting as low as ~ 15 K between a Γ_5 ground state and a Γ_1 first excited state. If there were a large Schottky contribution due to this CEF splitting in the temperature range of the high temperature fit to $C(T)$, the values of γ and Θ_D determined from the fit would be altered. Based on the CEF fits to the $\chi_{dc}(T)-\chi_0$ data, the worst case scenario (which would lead to the largest possible change in γ) occurs for a splitting of 23 K. The resulting Schottky contribution to the specific heat would result in a reduced γ (50 mJ/mol K^2) and a slightly lower Θ_D (246 K). Since the CEF contribution to $C(T)$ is not significant below 1.6 K for splittings above 15 K, the large value of γ (~ 1 J/mol K^2) determined from the low temperature fit to $C(T)$ is not affected by potential CEF effects. The various acceptable CEF splitting schemes do not significantly alter the magnetic entropy release of 90% $R \ln 3$ by 8 K, which remains in support of a triplet ground state.

A schematic representation of the $(H-T)$ phase diagram for $PrOs_4As_{12}$ (Fig. 7), is shown in Fig. 6(a). The vertical line labeled "b" in the schematic phase diagram represents an $M(H)$ measurement at $T=0.425$ K shown in Fig. 6(b). The points H_1 and H_2 along line b are features in the $M(H)$ data, which are defined using the derivative dM/dH shown in Fig. 6(d) as a function of H. The horizontal line labeled "c" represents an $M(T)$ measurement at $H=1.5$ T [Fig. 6(c)]. The features at T_1 and T_2 along c are defined from the $M(T)$ data shown in Fig. 6(c). Similar features in the other $M(H,T)$ measurements were used to generate the full $H-T$ phase diagram for $PrOs_4As_{12}$ shown in Fig. 7. The error bars are rough estimates of the transition widths, based upon the widths of features in the derivatives of $M(H)$ [Fig. 6(d)] and $M(T)$ (not shown). It may be inferred from the features in the
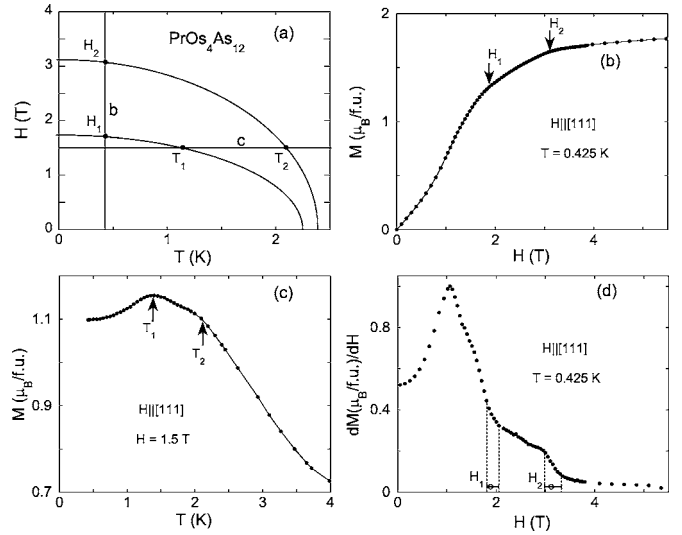

FIG. 6. (a) Schematic representation of the $PrOs_4As_{12}$ magnetic field–temperature $(H-T)$ phase diagram. The vertical and horizontal lines represent isothermal $M(H)$ and constant field $M(T)$ measurements as depicted in (b) and (c). (b) Magnetization M vs H at 0.425 K, with features at H_1 and H_2 used to define the phase diagram. (c) Magnetization M vs T at 1.5 T, along with two clear features at T_1 and T_2, used to contrast the phase diagram. (d) The derivative dM/dH as a function of H indicates two features used to define H_1 and H_2 in Fig. 6(b). The dotted lines represent estimated transition widths for H_1 and H_2.

UCSD $C(T)$ data that there are two phase transitions. Thus, $PrOs_4As_{12}$ appears to have an AFM ground state, a second ordered state at intermediate T and H, and is paramagnetic at high T and H.

The AFM nature of the ground state is supported by several observations. The peak in $\chi_{dc}(T)$ is a traditional indication of the onset of AFM, which is also suggested by the lack of hysteresis in $M(H)$, and is compatible with a CEF-split Γ_5
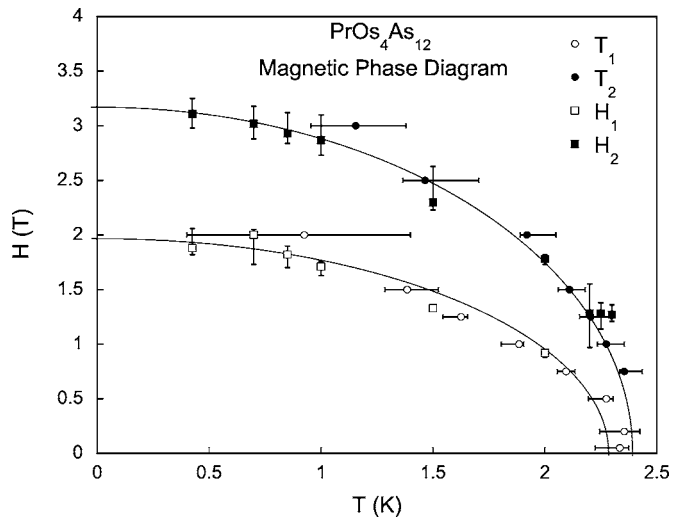

FIG. 7. Magnetic field-temperature $(H-T)$ phase diagram for $PrOs_4As_{12}$, as defined by features in the magnetization (Fig. 2) (circles and squares). The lines are guides to the eye.

magnetic triplet ground state. Furthermore, the suppression of the ground state order with H is consistent with AFM order. The nature of the second ordered phase is difficult to establish from the results of this study, but in light of the low-T behavior of other Pr-based filled skutterudites such as $PrFe_4P_{12}$,[5,6] magnetic or quadrupolar ordering seem to be likely possibilities. Recent neutron diffraction experiments on $PrOs_4As_{12}$ confirm that the low field ordered phase is antiferromagnetic.[28]

To summarize, magnetization and specific heat measurements on $PrOs_4As_{12}$ indicate the existence of at least two distinct phase transitions at temperatures below 2.3 K and in fields below 3 T. The magnetic behavior of the low temperature phase is consistent with AFM order. The electrical resistivity displays a sharp decrease due to the onset of ordering and has features consistent with Kondo lattice behavior. In the paramagnetic state, specific heat measurements indicate an electronic specific heat coefficient with $\gamma \approx 50-200$ mJ/mol K^2. In the antiferromagnetic state, an analysis of the $C(T)$ data yields a very large $\gamma \sim 1$ J/mol K^2 at low T ($T \lesssim 1.6$ K).

---

[1] M. B. Maple, E. D. Bauer, N. A. Frederick, P.-C. Ho, W. M. Yuhasz, and V. S. Zapf, Physica B **328**, 29 (2003).

[2] Y. Aoki, H. Sugawara, H. Hisatomo, and H. Sato, J. Phys. Soc. Jpn. **74**, 209 (2005).

[3] B. C. Sales, in *Handbook on the Physics and Chemistry of Rare Earths*, edited by K. A. Gschneidner Jr., J.-C. Bünzli, and V. K. Pecharsky (Elsevier Science, Amsterdam, 2003), Vol. 33, pp. 1–34.

[4] M. S. Torikachvili, J. W. Chen, Y. Dalichaouch, R. P. Guertin, M. W. McElfresh, C. Rossel, M. B. Maple, and G. P. Meisner, Phys. Rev. B **36**, 8660 (1987).

[5] Y. Aoki, T. Namiki, T. D. Matsuda, K. Abe, H. Sugawara, and H. Sato, Phys. Rev. B **65**, 064446 (2002).

[6] L. Hao, K. Iwasa, M. Nakajima, D. Kawana, K. Kuwahara, M. Kohgi, H. Sugawara, T. D. Matsuda, Y. Aoki, and H. Sato, Acta Phys. Pol. B **34**, 1113 (2003).

[7] T. D. Matsuda, H. Okada, H. Sugawara, Y. Aoki, H. Sato, A. V. Andreev, Y. Shiokawa, V. Sechovsky, T. Honma, E. Yamamoto, and Y. Ōnuki, Physica B **281-282**, 220 (2000).

[8] H. Sugawara, T. D. Matsuda, K. Abe, Y. Aoki, H. Sato, S. Nojiri, Y. Inada, R. Settai, and Y. Ōnuki, Phys. Rev. B **66**, 134411 (2002).

[9] T. Tayama, J. Custers, H. Sato, T. Sakakibara, H. Sugawara, and H. Sato, J. Phys. Soc. Jpn. **73**, 3258 (2004).

[10] M. B. Maple, E. D. Bauer, V. S. Zapf, E. J. Freeman, and N. A. Frederick, Acta Phys. Pol. B **32**, 3291 (2001).

[11] E. D. Bauer, N. A. Frederick, P.-C. Ho, V. S. Zapf, and M. B. Maple, Phys. Rev. B **65**, 100506(R) (2002).

[12] M. B. Maple, P.-C. Ho, V. S. Zapf, N. A. Frederick, E. D. Bauer, W. M. Yuhasz, F. M. Woodward, and J. W. Lynn, J. Phys. Soc. Jpn. Suppl. **71**, 23 (2002).

[13] Y. Aoki, A. Tsuchiya, T. Kanayama, S. R. Saha, H. Sugawara, H. Sato, W. Higemoto, A. Koda, K. Ohishi, K. Nishiyama, and R. Kadono, Phys. Rev. Lett. **91**, 067003 (2003).

[14] K. Izawa, Y. Nakajima, J. Goryo, Y. Matsuda, S. Osaki, H. Sugawara, H. Sato, P. Thalmeier, and K. Maki, Phys. Rev. Lett. **90**, 117001 (2003).

[15] T. Cichorek, A. C. Mota, F. Steglich, N. A. Frederick, W. M. Yuhasz, and M. B. Maple, Phys. Rev. Lett. **94**, 107002 (2005).

[16] M. B. Maple, P.-C. Ho, N. A. Frederick, V. S. Zapf, W. M. Yuhasz, and E. D. Bauer, Acta Phys. Pol. B **34**, 919 (2003).

[17] E. E. M. Chia, M. B. Salamon, H. Sugawara, and H. Sato, Phys. Rev. Lett. **91**, 247003 (2003).

[18] P.-C. Ho, N. A. Frederick, V. S. Zapf, E. D. Bauer, T. D. Do, M. B. Maple, A. D. Christianson, and A. H. Lacerda, Phys. Rev. B **67**, 180508(R) (2003).

[19] M. Kohgi, K. Izawa, M. Nakajima, N. Metoki, A. Araki, N. Bernhoeft, J. M. Mignot, A. Gukasov, H. Sato, Y. Aoki, and H. Sugawara, J. Phys. Soc. Jpn. **72**, 1002 (2003).

[20] Z. Henkie (unpublished).

[21] G. M. Sheldrick, in *Program for the Solution of Crystal Structures* (University of Göttingen, Germany, 1985).

[22] G. M. Sheldrick, in *Program for Crystal Structure Refinement* (University of Göttingen, Germany, 1987).

[23] D. J. Braun and W. Jeitschko, J. Solid State Chem. **32**, 357 (1980).

[24] B. C. Sales, D. Mandrus, B. C. Chakoumakos, V. Keppens, and J. R. Thompson, Phys. Rev. B **56**, 15081 (1997).

[25] B. C. Sales, B. C. Chakoumakos, D. Mandrus, J. W. Sharp, N. R. Dilley, and M. B. Maple, Mater. Res. Soc. Symp. Proc. **545**, 13 (1999).

[26] C. Sekine, T. Uchiumi, I. Shirotani, and T. Yagi, Phys. Rev. Lett. **79**, 3218 (1997).

[27] G. P. Meisner, G. R. Stewart, M. S. Torikachvili, and M. B. Maple, in *Proceedings of the 17th International Conference on Low Temperature Physics, LT-17*, edited by U. Eckern, A. Schmid, W. Weber, and W. Wühl (Elsevier, Amsterdam, 1984), p. 711.

[28] M. B. Maple, N. P. Butch, N. A. Frederick, P.-C. Ho, J. R. Jeffries, T. A. Sayles, T. Yanagisawa, W. M. Yuhasz, S. K. McCall, M. W. McElfresh, M. J. Flores, Songxue Chi, H. J. Kang, J. W. Lynn, Pengcheng Dai, Z. Henkie, and A. Pietraszko, Proc. Natl. Acad. Sci. U.S.A. (to be published).

[29] M. B. Maple, E. D. Bauer, V. S. Zapf, and J. Wosnitza: in *Superconductivity in Nanostructures, High T_C and Novel Superconductors, Organic Superconductors*, edited by K. H. Bennemann and J. B. Ketterson, The Physics of Superconductors, Vol. II (Springer-Verlag, Berlin, 2004), Chap. 8, p. 555.

[30] W. M. Yuhasz, T. A. Sayles, P.-C. Ho, T. Yanagisawa, and M. B. Maple (unpublished).

[31] I. Shirotani, T. Uchiumi, K. Ohno, C. Sekine, Y. Nakazawa, K. Kanoda, S. Todo, and T. Yagi, Phys. Rev. B **56**, 7866 (1997).